Journal of Physics: Conference Series

Ferromagnetism in Mn-implanted Ge/Si nanostructure material

To cite this article: I T Yoon *et al* 2009 *J. Phys.: Conf. Ser.* **153** 012069

Journal of Physics: Conference Series **153** (2009) 012069 doi:10.1088/1742-6596/153/1/012069

Ferromagnetism in Mn-implanted Ge/Si nanostructure material

I. T. Yoon[1], C. J. Park, and T. W. Kang

Quantum Functional Semiconductor Research Center, Dongguk University, Seoul, 100-715 Korea

ityoon@dongguk.edu

Abstract. Multistacked Ge quantum dots (QDs) with Si spacers of different thicknesses have been grown on (100) Si substrates by rapid thermal chemical vapor deposition followed by Mn ion implantation and post-annealing. The presence of a ferromagnetic structure was confirmed in the insulating $(Si_{0.45}Ge_{0.55})Mn_{0.03}$ diluted magnetic quantum dots (DMQD) and semiconducting $(Si_{0.45}Ge_{0.55})Mn_{0.05}$ DMQD. The DMQD materials were found to be homogeneous, and to exhibit p-type conductivity and ferromagnetic ordering with Curie temperatures $T_C = 350$ and 160 K respectively. The x-ray diffraction (XRD) data show that there is a phase separation of Mn_5Ge_3 from the MnGe nanostructure. Temperature-dependent electrical resistivity in the semiconducting DMQD material indicates that manganese introduces two acceptor levels in germanium at 0.14 eV from the valence band and 0.41 eV from the conduction band implying that Mn substitutes for Ge. Therefore, it is likely that the ferromagnetic exchange coupling of DMQD material with T_C = 160 K is hole-mediated due to formation of bound magnetic polarons and the ferromagnetism in the sample with $T_C > 300$ K is due to Mn_5Ge_3 phase.

1. Introduction

Diluted magnetic semiconductors (DMSs), often referred to as semi-magnetic semiconductors, based on III-V semiconductors have attracted a great deal of attention recently because of their potential application in spintronic devices that exploit the charge and spin of electrons [1]. The lattices of these materials consist of magnetic ions partially substituting for some of the cations, thereby inducing a local magnetic moment in the lattice and donating carriers into the system. The ferromagnetic nature of these materials is caused by the exchange interaction between localized magnetic moments introduced by the magnetic ions and the carrier spins. Therefore, for device applications, it is desirable to find materials that exhibit ferromagnetism at as high a temperature as possible. Since Dietl et al. [2] predicted that wide band-gap DMS materials, such as GaMnN and ZnMnO, can have Curie temperatures (T_c) above room temperature, based on the mean-field Zener model of ferromagnetism, several materials with Curie temperatures greatly above room temperature have been found in many studies [3-8]. In particular, group-IV-based DMS materials [9-13] with high Curie temperatures have attracted much attention because of their compatibility with conventional semiconductor integrated circuit manufacturing techniques since Park et al. reported an epitaxially grown single crystal of

[1]To whom any correspondence should be addressed.

Mn_xGe_{1-x} (x = 3.5%) with a magnetically ordered phase and a Curie temperature up to 116 K because of a long-range ferromagnetic interaction [9]. The structural, electronic, and magnetic properties for Si_xGe_{1-x} alloys doped with Mn have been investigated theoretically and experimentally [14-17]. In this paper, we report on the magnetic and transport properties of $(Si_{0.45}Ge_{0.55})Mn_{0.05}$ diluted magnetic quantum dots (DMQD), formed through ion implantation and post-annealing. Energy dispersive x-ray fluorescence (EDX), x-ray diffraction (XRD), atomic force microscopy (AFM), high-resolution transmission electron microscopy (HRTEM)**,** superconducting quantum interference device (SQUID), Hall effect and Raman measurements were performed to characterize the samples.

2. Experimental

Ten and twenty-stacked Ge QDs with Si spacers of different thicknesses were grown on *p*-type (100) Si substrates by rapid thermal chemical vapor deposition (RTCVD) with a base pressure of 2×10^{-7} Torr using SiH_4 and GeH_4 as Si and Ge source gases. The QD multilayers consisted of ten and twenty bilayers, each of which was composed of 6.5 monolayers of Ge and a Si-spacer layer of 14–100 nm in thickness. The samples underwent the following growth procedures: the Ge quantum dots (QDs) were deposited in the Stranski-Krastanow (SK) growth mode. After baking at 1000 °C in hydrogen, ten and twenty layers of self assembled Ge QDs with 44 and 59 nm-thick Si barrier (hereafter referred as samples A and B) were grown on a 200 nm-thick Si buffer layer at 700 °C with a pressure of 100 mTorr. The Ge QD samples A and B grown by RTCVD were uniformly implanted with Mn^+ ions at an energy of 200 keV and a dose of 2.5 x 10^{16} and 5 x 10^{16} cm^{-2}, respectively. After implantation, thermal annealing was performed at 650 ^oC under Ar gas at ambient pressure for 10 minutes in a rapid thermal annealing (RTA) furnace to recover the damage. XRD and AFM were employed to analyze the structural and morphological properties of the annealed samples. Hysteresis loops were measured at temperatures in the range 4 - 300 K using a SQUID, and a high-sensitivity (10^{-8} emu) alternating gradient magnetometer (AGM). In all the measurements, the magnetic field was applied parallel to the sample surface. The concentration of Mn in the sample A and B using an EDX was determined at around 3.0 and 5.0%**,** respectively. The grown sample doped with manganese exhibited p-type conductivity in Hall effect measurements. The hole concentration and resistivity of the $(Si_{0.45}Ge_{0.55})Mn_{0.03}$ sample A was determined to be 1×10^{14} cm^{-3} and 1.7×10^4 Ω cm, respectively. The hole concentration and resistivity of the $(Si_{0.45}Ge_{0.55})Mn_{0.05}$ sample B was determined to be 1×10^{15} cm^{-3} and 1.2×10^3 Ω cm, respectively.

3. Results and discussion

Fig. 1 shows the XRD patterns of the as-grown and annealed samples A and B. Si(002) and Si(004) substrate peaks can be observed from the as-grown sample. The XRD spectra for the annealed samples A and B are similar, containing a dominant Mn_5Ge_3 phase. This phase is known to have a theoretical Curie temperature above room temperature [18].

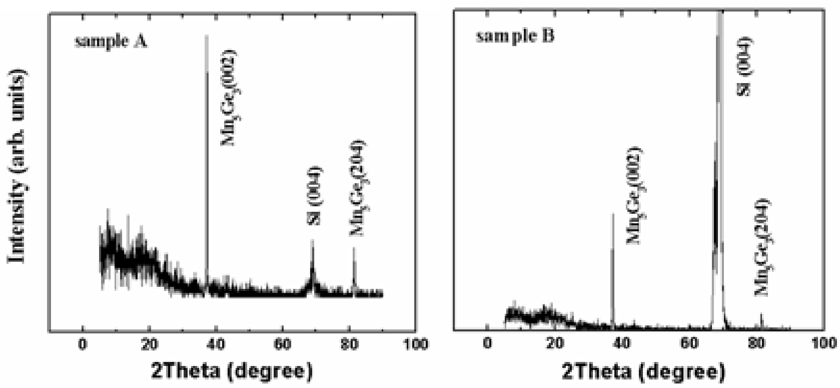

Fig. 1. XRD spectrum for the samples A and B after thermal annealing for 10 min.

Fig. 2 shows cross-sectional HRTEM images of ten and twenty stacked Ge QDs with 44 and 59 nm-thick Si barriers. The density of the dots was approximately 2×10^8 cm^{-2}. They demonstrate that the Ge QDs are vertically ordered and fully contrasted with the Si spacer. No misfit dislocations were observed from the TEM images. The height and the base of the dots range from 8 to 15 nm and from 140 to 200 nm, respectively.

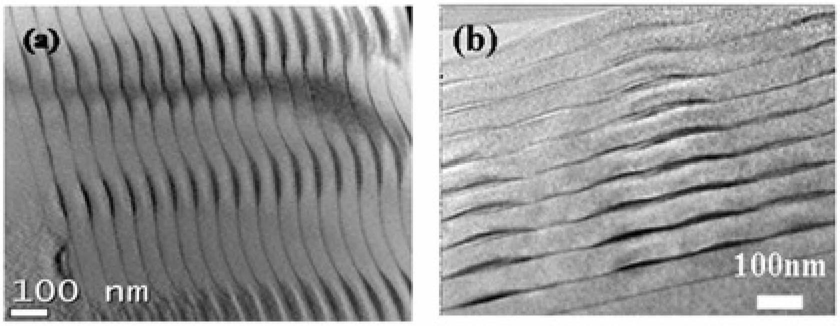

Fig. 2. Cross-sectional HRTEM images of twenty and ten-stacked Ge QDs with Si spacers of (a) 59 nm and (b) 44 nm in thickness.

Fig. 3(a) and (b) shows the AFM 2 μm image of samples A and B, respectively. It is noted that some DMQDs seem to merge into a single large QD. The DMQDs can still be seen after the thermal annealing process.

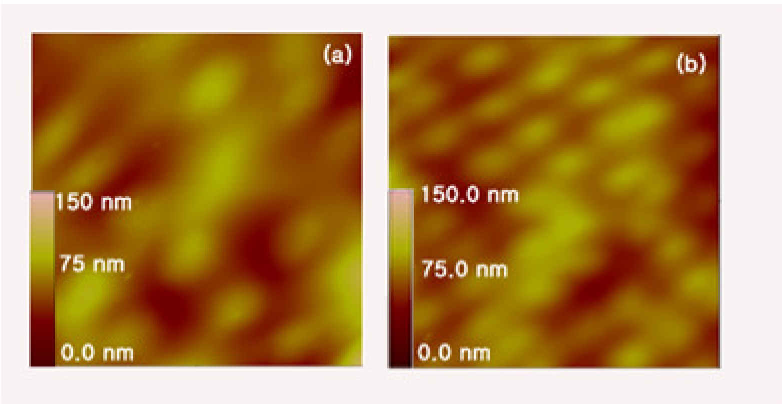

Fig. 3. Fig. 3(a) and (b) shows the AFM 2 μm image of samples A and B, respectively.

Fig. 4 shows the magnetic field-dependent magnetization, M, at 5 K for DMQD samples A and B after RTA for 10 min, with the magnetic field applied parallel to the plane of the film using an AGM. Clearly elongated hysteresis loops are observed in Fig. 4, indicating that ferromagnetic ordering is present; the diamagnetic background of the substrate was subtracted from the data. The samples showed coercivities in the range 40 ~ 60 Oe. The magnitude of hysteresis of sample B is greater than that of the sample A because of the increased Mn concentration.

The temperature dependence of the magnetization curve, M(T), for DMQD samples A and B are presented in Fig. 5. A negative magnetization signal is shown up to 350 K for sample A. Squares in Fig. 5 denote the magnetization of the insulating sample A. It can be determined that the Curie temperature for the sample A is around 350 K whereas the Curie temperature for the semiconducting sample B is around 160 K. The observed temperature-dependent magnetization curve M(T) for samples A and B appears to be very different from the usual convex M(T) curve expected from the

Weiss mean-field theory [19]. The temperature-dependent magnetization shows an unusual outwardly concave shape that is consistent with the behaviour of a GeMn system [9], suggesting a signature of charge carrier localization. It has been shown that such a non-mean-field like behaviour in M(T) curves is much more typical of semi-insulating DMS systems than metallic ones [20-21].

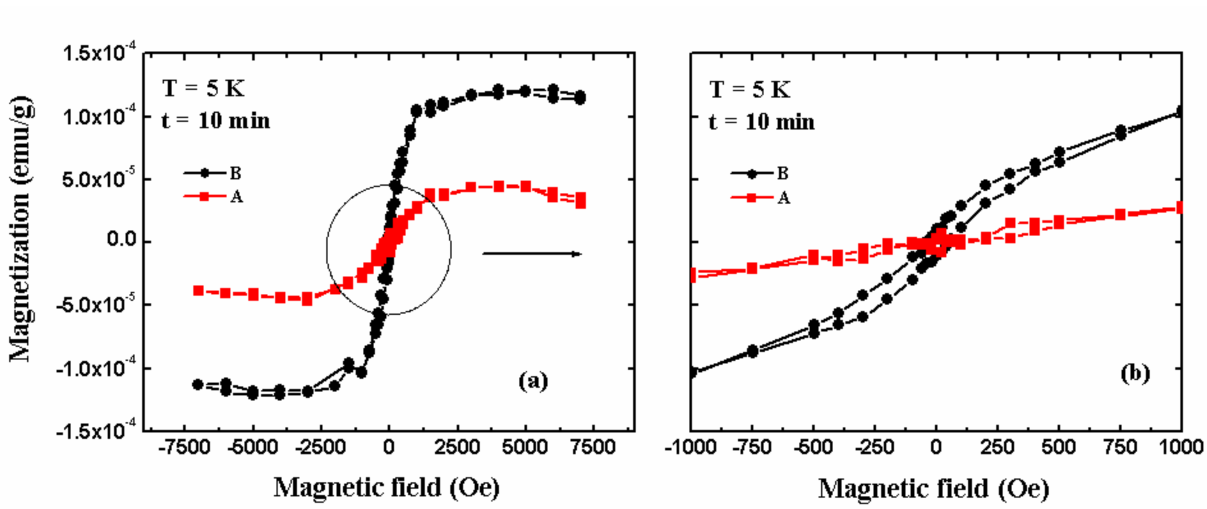

Fig. 4. (a) A ferromagnetic hysteresis loop at 5 K for DMQD samples A and B after thermal annealing for 10 min. The solid line serves as a visual guide (b) Magnified view of the hysteresis loop.

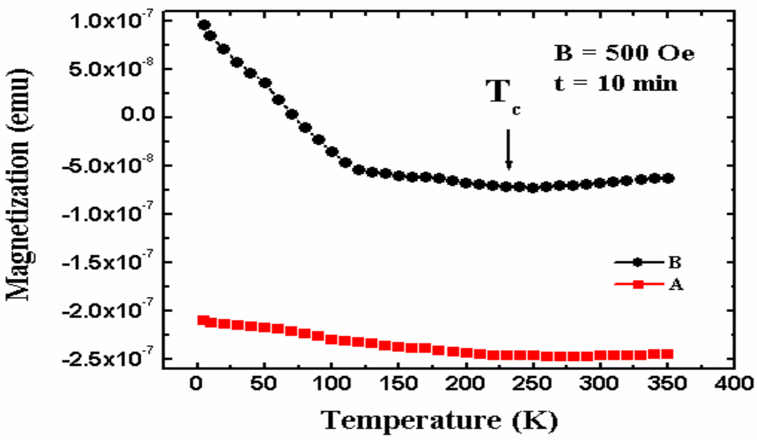

Fig. 5. Temperature dependence of magnetization for DMQD sample A and B after thermal annealing for 10 min. obtained by SQUID magnetometry with a magnetic field of 500 Oe.

Fig. 6 shows the electrical resistivity as a function of temperature for the sample A. As can be seen from Fig. 6, the resistance increases with decreasing temperature, which is also typical semi-insulating behaviour. The rate of resistance change can be divided into two regions. The temperature-dependent resistance was fitted with an Arrhenius function $\rho = \rho_0 \exp(\varepsilon_a/kT)$ where ε_a is the activation energy. Low lying levels at 0.05 and 0.01 eV from the valence band could be observed in Fig. 6. The source of these levels could not be ascertained; it does not seem to be directly related to the manganese [22] except clusters. We assumed that these differences in magnetic behaviour between samples A and B were due to the differences in electrical properties. They show clearly that both the semiconducting and insulating samples were ferromagnetic. Given the highly insulating nature of sample A, no itinerant hole based picture is possible, and so the RKKY-type scenario discussed extensively in the framework of GaMnAs magnetization [1,2] simply does not apply to sample A. However, the XRD spectra for the annealed sample A containing a dominant Mn_5Ge_3 phase indicates that the ferromagnetism of the sample is due to this phase.

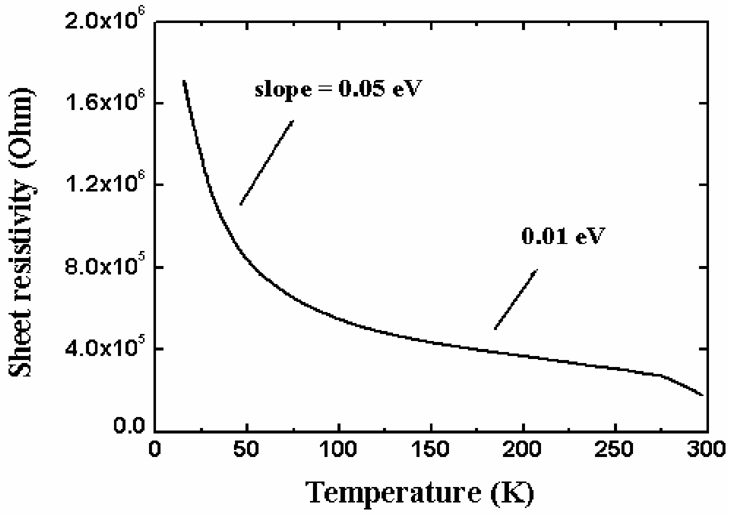

Fig. 6. Electrical sheet resistivity of DMQD sample A as a function of temperature.

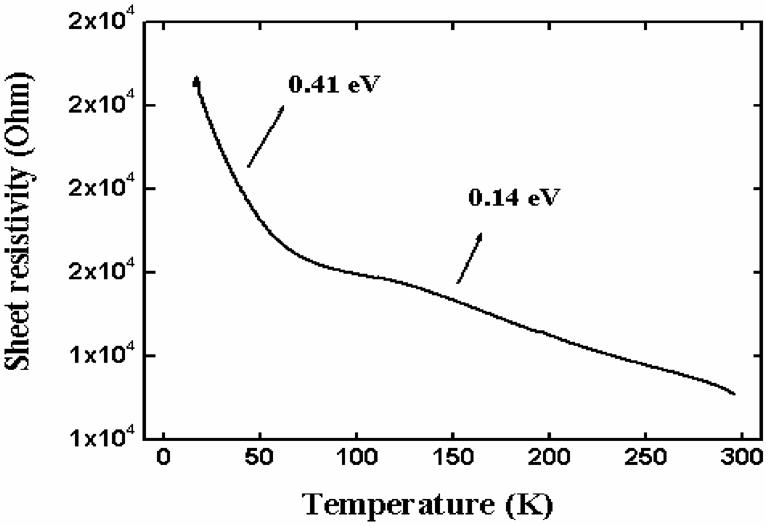

Fig. 7. Electrical sheet resistivity of DMQD sample B as a function of temperature.

Fig. 7 represents the electrical resistivity as a function of temperature for sample B. As can be seen from Fig. 7, the resistance increases with decreasing temperature, which is a typical semiconducting characteristic. The strong divergence at low temperature indicates strong carrier localization behaviour. The temperature-dependent resistance was also fitted with an Arrhenius function. Low lying levels at 0.41 eV and 0.14 eV from the valence band could be observed in Fig. 7. The activation barrier associated with the separation between the Mn acceptor level and Ge valence band is known to be ~ 160 meV in p-type Mn-doped Ge crystal and the activation barrier between the Mn acceptor and conduction band is known to be ~ 390 meV in n-type Mn-doped Ge crystals from the temperature-dependent resistivity measurements [22]. It is possible that Mn is also incorporated into the Si matrix. The reason why the activation energies are not associated with Si is that the Mn-related double donor level, which comes from Mn atoms occupying Si sites in p-type conditions, is around

0.29 eV above the valence band [23].According to Woodbury et al.[22], at low temperatures the exponential regimes with activation energies of 140 meV and 410 meV are most likely associated with a shallow acceptor level of Mn substituting Ge suggesting that the transport is dominated by a thermal activation mechanism. Therefore, the ferromagnetism observed in sample B with T_C = 160 K is associated with the carriers produced by Mn atoms occupying Ge sites (Mn_{Ge}), as confirmed by transport measurements. This behaviour further suggests that the ferromagnetic exchange coupling is hole-mediated, but the hole concentration of sample B was only ~10^{15} cm^{-3}, which is too low to show hole-mediated ferromagnetism. However, the concentration of localized carriers residing in the impurity band is not too low. Therefore, the bound magnetic polaron (BMP) percolation picture [20,21] as discussed in the framework of strongly semi-insulating DMS materials may be relevant. In this picture, the spin of localized carriers polarizes the surrounding magnetic impurities, leading to the so-called bound magnetic polarons [24]. Alignment of the polarization is mediated by the localized holes in the system via interaction according to the RKKY theory [2]. We consider that the ferromagnetism of sample B is due to the magnetic polarons, indicating that room temperature ferromagnetism in IV group semiconductors doped with Mn can be realized in the future.

4. Conclusion

In summary, DMQD has been formed through Mn ion implantation and thermal annealing. It was found that manganese introduces two acceptor levels in germanium at 0.14 eV from the valence band and 0.41 eV from the conduction band, implying Mn substituting Ge. Therefore, it can be concluded that the ferromagnetic exchange coupling of the semiconducting sample with a Curie temperature around 160 K is hole-mediated due to formation of bound magnetic polarons. On the other hand, the ferromagnetism in the insulating sample (with a Curie temperature over 300 K) is associated with the dominant Mn_5Ge_3 phase.

Acknowledgements

This work was supported in part by funds from the Quantum-functional Semiconductor Research Center and Dongguk University and by the Korea Science and Engineering Foundation (KOSEF) grant funded by the Korea government (MOST) in 2008.

References

[1] Ohno H 1998 *Science* **281** 951
[2] Dietl T, Ohno H, Matsukura H, Cibert J and Ferrand D 2000 *Science* **287** 1019
[3] Matsumoto Y, Murakami M, Shono T, Hasegawa T, Fukumura T, Kawasaki M, Ahmet P, Chihyow T, Koshihara S and Koinuma H 2001 *Science* **291** 854
[4] Hartman T, Lampalzer M, Klar P J, Stolz W, Heimbrodt W, Keug von Nidda H–A, Loids A and Svistov L 2002 *Physica E* **13** 572
[5] Theodoropoulou N, Hebard A F, Overberg M E, Abernathy C R, Pearton S J, Chu S N G and Wilson R G 2002 *Phys. Rev. Lett*. **89** 107203-1
[6] Medvedkin G A, Ishibashi T, Nishi T, Hayata K, Hasegawa Y and Sato K 2000 *Jpn. J. Appl. Phys*. Part 2 **39** L949
[7] Reed M L, El-Masry N A, Stadelmaier H H, Ritums M K, Reed M J, Parker C A, Roberts J C and Bedair S M 2001 *Appl. Phys. Lett*. **79** 3473
[8] Sonoda S, Shimizu S, Sasaki T, Yamamoto Y and Hori H 2002 *J. Cryst. Growth* **237-239** 1358
[9] Park Y D, Hanbicki A T, Erwin S C, Hellberg C S, Sullivan J M, Mattson J E, Ambrose T F, Wilson A, Spanos G and Jonker B T 2002 *Science* **295** 651
[10] Cho S, Choi S, Hong S C, Kim Y, Ketterson J B, Kim Y C and Jung J H 2002 *Phys. Rev. B* **66** 033303
[11] Nakayama H, Ohta H and Kulatov E 2001 *Physica B* **302–303** 419
[12] Zhang F M, Liu X C, Gao J, Wu X S, Du Y W, Zhu H., Xiao J Q and Chen P 2005 *Appl.*

Journal of Physics: Conference Series **153** (2009) 012069 doi:10.1088/1742-6596/153/1/012069

Phys. Lett. **85** 786
[13] Bolduc M, Awo-Affouda C, Stollenwerk A, Huang M B, Ramos F G, Agnello G and LaBella V P 2005 *Phys. Rev. B* **71** 033302
[14] Peressi M, Debernardi A, Picozzi S, Antoniella F and Continenza A 2005 *Computational MaterialsScience* **33** 125
[15] Picozzi S, Antoniella F, Continenza A, MoscaConte A, Debernardi A and Peressi M 2004 *Phys. Rev B* **70** 165205
[16] Yu S S, Cho Y M, Ihm Y E, Kim D J, Kim H J, Hong S K, Oh S J, Woo B C and Kim C S 2006 *Current Appl. Phys.* **6** 478
[17] Stropa A, Picozzi S, Continenza A and Freeman A J 2003 *Phys. Rev. B* **68** 155203
[18] Yamada N, Maeda K, Usami Y and Ohoyama T 1986 *J. Phys. Soc. Jpn.* **55** 3721
[19] Kittel C *Introduction to Solid State Physics* Wiley, New York (1996)
[20] Sarma S D, Hwang E H and Kaminski A 2003 *Phys. Rev B* **67** 155201
[21] Kaminski A J and Sarma S D 2002 *Phys. Rev. Lett.* **88** 247202
[22] Woodbury H H and Tyler W W 1955 *Phys. Rev.* **100** 659
[23] Bernardini F, Picozzi S and Continenza A 2004 *Appl Phys Lett.* **84** 2289
[24] Chen J, Wang K L and Galatsis K 2007 *Appl. Phys. Lett.* **90** 012501